Hot Tearing Susceptibility of AA3000 Aluminum Alloy Containing Cu, Ti, and Zr

GHADIR RAZAZ and TORBJÖRN CARLBERG

Severe hot tearing has been observed during DC casting of modified AA3000 alloys with additions of Cu, Ti, and Zr, although these alloys are regarded as rather easy to cast. Extensive studies have been performed on both synthetic and industrial AA2000, AA6000, and AA7000 alloys, but less data are available for AA3000 alloys. This work was thus initiated to investigate the hot tearing susceptibility of AA3000 alloys with varying alloy element content using constrained rod casting molds. The results showed that the Cu and Fe content have a major impact on hot tearing resistance, while the effects of Zr and Ti are minor. Cu in a range from 0.3 to 1.2 wt pct significantly increased the hot tearing tendency. This is due to the existence of high eutectic fractions at low temperatures, as well as porosity formation associated with bad feeding at the end of solidification. A strong cracking tendency was observed below an Fe content 0.2 wt pct owing to decreased precipitation of the Al_6(Mn, Fe) phase. It was found that primary Al_6(Mn, Fe) phases lead to early bridging between the grains, which reinforces the alloy during the vulnerable temperature range for hot tearing. Zr and Ti additions weakly enhanced or reduced hot tearing severity, respectively.

https://doi.org/10.1007/s11661-019-05290-1

I. INTRODUCTION

HEAT exchangers are an important application of direct chill (DC) cast rolling ingots produced from AA3000 Al alloys. To optimize the material properties for these applications, copper alloying is common, as well as minor additions of titanium and zirconium. These additions are mainly made to improve the corrosion properties, which is very important for automotive heat exchangers, but the modifications have also resulted in a marked increase in hot tearing tendency, which differs from what had previously been experienced for AA3000 alloys with regular compositions.

Hot tearing is a serious defect that occurs during the solidification of Al alloys in DC casting. It is an irreversible failure, which starts forming during the semi-solid stage of solidification and eventually shows up as a crack either on the surface or inside the solidified ingots. These cracks are usually visible to the naked eye, and the ingots must be scrapped to prevent failures in further processing.[1–3] Studies of hot tearing have resulted in several theories about the mechanisms of crack nucleation and propagation involving metallurgical and thermo-mechanical factors. The key factors for hot tearing are liquid film and inadequate eutectic feeding in the last stage of solidification, together with thermally induced stress-strain, which cannot be accommodated by the semi-solid material.[1,4–7]

Hot tearing susceptibility (HTS) is highly dependent on the chemical compositions of Al alloys, and is described as a lambda curve for binary alloys. In most binary alloys, an initial increase in solute content (start of the lambda curve) enlarges the solidification interval. As a result, the alloys spend more time in a vulnerable stage for hot tearing (between 90 and 99 pct solid), and thus are prone to cracking. With further addition of solute, the hot tearing tendency decreases due to a higher eutectic fraction. Better interdendritic liquid feeding during shrinkage allows the cracks to heal (second half of lambda curve).[1,3,4] Chemical composition can also influence the hot tearing resistance of alloys by changing the morphology, precipitation, and grain size. However, contradictory results related to hot tearing have been reported. For instance, it is believed that grain refining increases the hot tearing resistance by reducing the grain size, altering the grain morphology from columnar to equiaxed, and decreasing the film thickness between the grains.[1,5,7] However, Easton *et al.*[6] state that refined grain size reduces the permeability of the mush and enhances the hot tearing tendency.[1,6]

GHADIR RAZAZ and TORBJÖRN CARLBERG are with the Department of Natural Science, Mid Sweden University, 851 70 Sundsvall, Sweden. Contact e-mails: Ghadir.razaz@miun.se; Torbjorn.carlberg@miun.se

Manuscript submitted February 7, 2019.
Article published online May 21, 2019

Besides the chemical composition, process variables such as mold and melt temperature[1] and melt quality[8] affect the HTS. Hot tearing can be propagated in both intergranular and transgranular paths, and is favored by porosity and brittle secondary phases.[5,9]

The hot tearing mechanism in multicomponent Al alloys is more complex due to alloying element interactions, giving more complicated solidification paths.[2] As previously mentioned, industrial experience shows that new modifications of AA 3000 alloys with Cu and small additions of Ti and Zr cause strong hot tearing sensitivity. Hot tearing has been intensively studied for AA2000, AA6000, and AA7000 alloys,[1–16] while only limited data are available for AA3000 alloys.[17,18] This shows that more studies on hot tearing formation for the AA3xxx group are needed.

The aim of this work is to investigate the effect of alloying elements such as Cu, Fe, Ti, and Zr on the HTS of AA3xxx alloys. Therefore, alloys with various compositions in respect to these elements were produced using a constrained rod casting (CRC) mold. Direct observation was done to evaluate the HTS qualitatively, as well as microstructural investigation at hot cracking positions. Attention was paid to parameters such as morphology, secondary phase formation, and grain size.

Table I. Chemical Compositions of the Alloys from Group A (Weight Percent)

Alloys	Mn	Fe	Cu	Ti	Zr	B
A1	1.52	0.13	0.35	0.14	0.005	0.0007
A2	1.51	0.12	0.35	0.14	0.002	0.001
A3 (Base Alloy)	1.45	0.2	0.34	0.15	0.005	0.002
A4	1.45	0.29	0.34	0.14	0.006	0.003
A5	1.39	0.2	0.78	0.16	0.002	0.002
A6	1.36	0.2	0.33	0.18	0.07	0.002

Table II. Chemical Compositions of the Alloys from Group B (Weight Percent)

Alloys	Mn	Fe	Cu	Ti	Zr	B
B1	1.42	0.14	0.03	0.02	0.09	0.0001
B2	1.27	0.13	0.32	0.02	0.08	0.0003
B3	1.4	0.12	0.74	0.02	0.1	0.0001
B4	1.39	0.12	1.28	0.02	0.1	0.0001
C1	1.61	0.19	0.12	0.01	0.13	0.0002
C2	1.58	0.19	0.13	0.01	0.02	0.0002
C3	1.6	0.18	0.3	0.01	0.11	0.0005
D1(Base Alloy)	1.7	0.24	0.72	0.04	0.12	0.001
D2	1.7	0.24	0.7	0.22	0.12	0.003

II. EXPERIMENTAL PROCEDURE

A. *Materials*

The chemical compositions of the 3xxx aluminum alloys used in this work are given in Tables I and II. It should be mentioned that alloys A1, A3, B1, C1, C2, C3, and D1 were obtained from the industry. The composition of these alloys was then modified by adding Fe, Cu, Zr, Ti, and grain refiner, respectively, to obtain the other alloys.

In Table I, alloys A1 to A4 are designed to study the effect of varying Fe contents. In alloy A5, the Cu content is increased in an alloy with normal Fe content, and in A6 the Zr content is increased in an alloy with normal Fe and Cu contents. In Table II, the alloys B1 to B4 and alloys C1 and C3 are designed to study effects of varying Cu contents in alloys containing Zr. In alloy C2 the Zr addition is omitted. In the D1 and D2 alloys, the effects of different Ti additions were studied.

B. *Evaluation of Hot Tearing Susceptibility*

A CRC mold was used to evaluate HTS. During casting with a CRC mold, stress is induced in the rods due to constrained shrinkage, which may lead to hot tearing.[19] Figure 1(a) shows the design of the CRC mold. A sample after casting is shown in Figure 1(b). The mold cavity allows four rods to be cast with a diameter of 9.5 mm, and lengths of 51, 89, 127, and 165 mm, respectively. The rods are constrained against free contraction by the sprue at one end and by a ball with a diameter of 19 mm at the other end. The mold was normally preheated to a temperature of 330 °C before each cast, but some tests were also carried out with a mold temperature of 500 °C to obtain a slower cooling rate. 420 g of each alloy was melted in a crucible at a furnace temperature of 800 °C. After 60 minutes, alloy additions were made and the crucible was returned to the furnace for a further 30 minutes before the melt was poured into the preheated mold. The casting was removed from the mold after 5 minutes. Three castings were carried out for each alloy, following the same procedure. To confirm the compositions of the alloys, slices were taken from the sprue for each casting and analyzed by optical emission spectroscopy (OES).

Hot tears in the samples were inspected by eye. The degree of hot tearing severity was classified into four categories: short hairline, full hairline, crack and half broken rod. The HTS was then calculated using Eq. [1].[19,20]

$$HCS = \sum f_{\text{crack}} f_{\text{length}} f_{\text{location}}. \quad [1]$$

In Eq. [1],[19,20] f_{crack}, f_{length}, and f_{location} are factors for crack severity, rod length, and crack location, respectively. The values of each factor are given in Table III.

C. *Direct Chill Casting Simulator*

The DC simulator is designed to produce a casting structure with the same variations in solidification conditions on the surface and the interior as normally produced ingots. The apparatus is shown in Figure 2 and is composed of an insulating tube made of alumina. The casting is made in a slightly tapered hole, with a length and diameter of 45 and 20 mm. The tube stands on a steel plate, which is removable. A water jet can be directed toward the steel plate.[21]

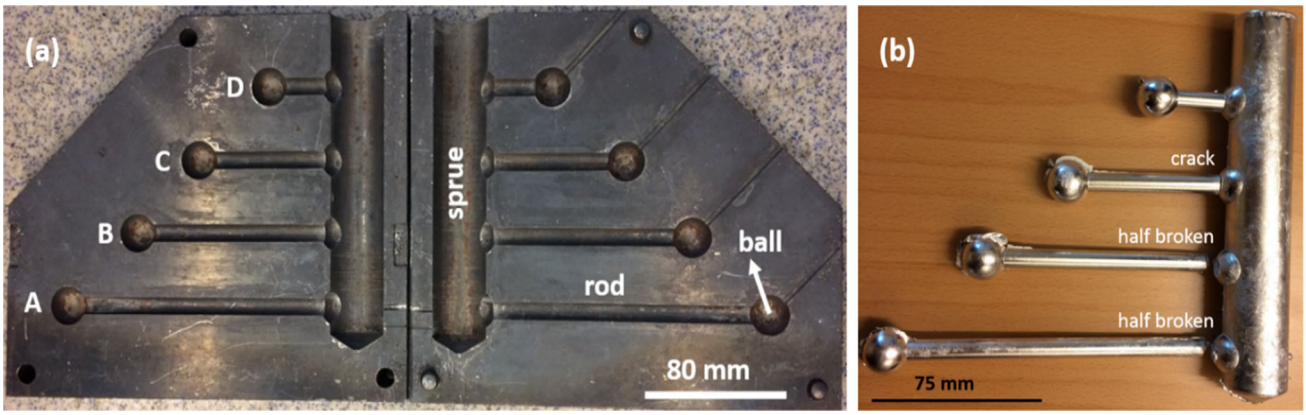

Fig. 1—(*a*) Steel mold for constrained rod casting, (*b*) image of a sample cast with the CRC mold showing cracks.

Table III. Hot Tearing Index Factors

Cracking Severity	f_{crack}	Length (rod)	f_{length}	Location	$f_{location}$
Short Hairline	1	rod A (longest)	4	at sprue	1
Full Hairline	2	rod B (second longest)	8	at ball	2
Crack	3	rod C (third longest)	16	middle of rod	3
Half Broken	4	rod D (shortest)	32		

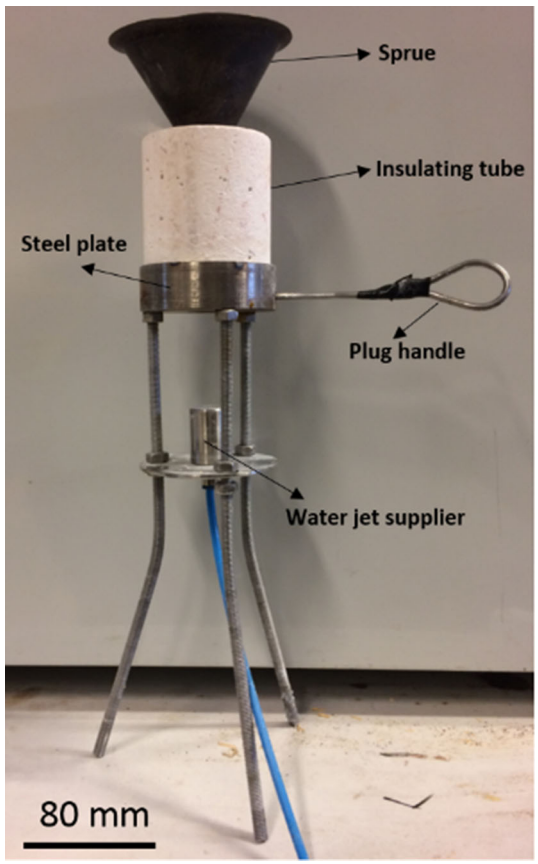

Fig. 2—Image of the direct chill cast simulator (DC simulator).

To produce samples with the DC casting simulator, 40 g of alloys A2, A3, and D1 were melted in a crucible at a furnace temperature of 700 °C. The melt was kept at that temperature for 20 minutes before being poured into the preheated tube (700 °C). Ten seconds after pouring the melt into the tube, water was sprayed for 30 seconds on the steel plate at a flow rate of 300 mL/min. Then, the plate was removed and water was sprayed directly on the bottom of the sample for 60 seconds. These two stages of cooling were intended to replicate the two steps of heat extraction in DC casting of an ingot that is, cooling in the mold followed by direct cooling. Cooling rate measurements and microstructure observations at a distance of 10 to 35 mm from the bottom of the sample exhibit good agreement with corresponding sections in DC cast ingots.

D. *Microstructure Analysis*

Representative samples were sectioned at the hot tearing positions and metallographically prepared. The polished samples were etched using 1 pct NaOH at 60 °C for 15 seconds. In addition, small pieces of alloys with a weight of 0.5 g were deep etched for 7 hours using a solution of 5 g of iodine and 50 ml of methanol to extract the intermetallic phases.[22] The samples were then examined by optical microscopy, scanning electron microscopy, SEM (MAIA3, Tescan), and energy-dispersive analyzer (EDX, AZtec) to characterize the morphology and intermetallic phases. Some samples were also anodized to observe the grain structure using polarized light. To measure the grain size, the number of

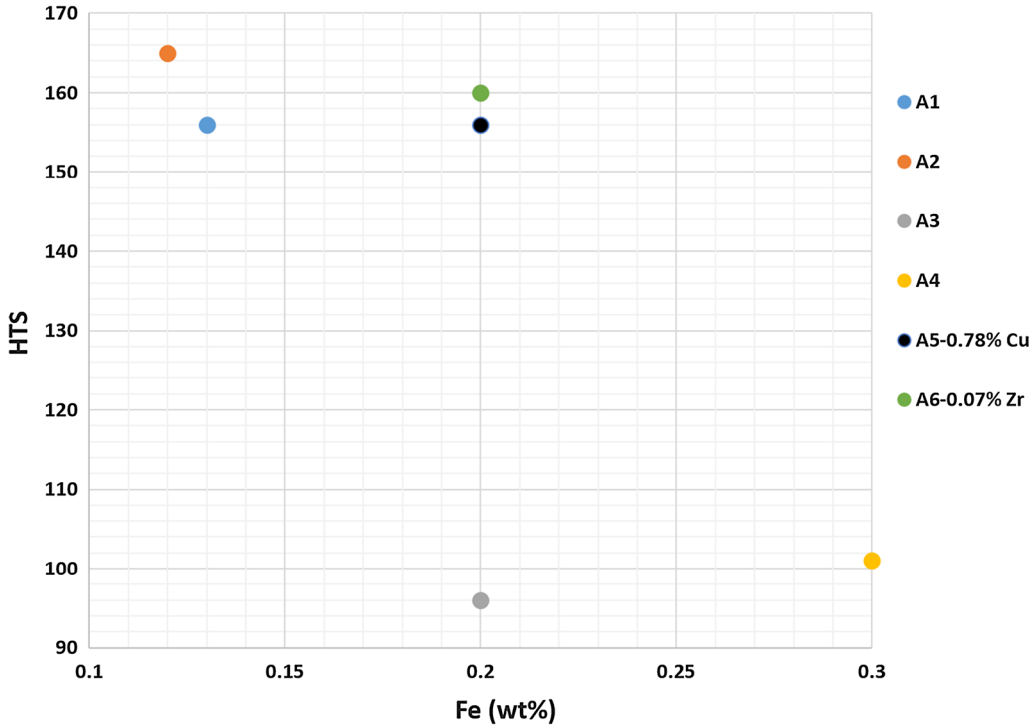

Fig. 3—Hot tearing susceptibility as a function of Fe content.

grain boundaries intersecting a circle of known circumference was counted. Fractured surfaces from the longest bars produced in the CRC molds were investigated in the SEM.

III. RESULTS

A. *Hot Tearing Indexation*

The HTS of AA3XXX alloys from group A with various Fe, Cu, Zr, and Ti content is shown in Figure 3. In the first four alloys (A1, A2, A3, and A4), the Fe content and the addition of grain refinement varied. Cu and Zr were added to create alloys A5 and A6, respectively, from an alloy with the original composition of alloy A3 (base alloy). It can be seen from Figure 3 that the HTS of alloys A3 and A4, with iron content of 0.2 and 0.29 wt pct, respectively, have similar and significantly lower crack tendency compared to A1 and A2 with 0.13 and 0.12 pct wt pct Fe, respectively. The results, therefore, clearly show that decreasing the Fe content below the normal 0.2 pct level increases crack sensitivity. This was also found for an AA6060 alloy in Reference 3. HTS for the low Fe alloys, that is, A1 (non-grain refined), and A2 (grain refined alloy) have approximately the same high crack sensitivity level. This means that in highly sensitive alloys, grain refining does not seem to decrease the risk of hot tearing.

Figure 3 shows that the tendency to crack has been significantly increased compared to the base alloy A3 for both alloys A5 and A6, which have additions of Cu (0.78 wt pct) and Zr (0.07 wt pct), respectively. This indicates a clear negative effect of Cu and Zr addition on crack resistance in this type of alloy.

Figure 4 shows the effect of Cu addition in the range of 0.03 to 1.28 wt pct on HTS. The general result is a significant increase in hot tearing severity with increased Cu content from alloy B1 with 0.03 wt pct, to alloy B4 with 1.28 wt pct Cu, and the HTS is substantially higher for all Cu alloys containing 0.3 pct or more. Thus, it can be concluded that addition of Cu has generally increased the crack severity in the investigated range.

The effect of Ti additions can be observed by comparing alloys D1 and D2. D2 with high Ti content (0.22 wt pct) shows no significant reduction in HTS compared to the base alloy D1 with 0.04 wt pct Ti. Thus, it can be concluded that the effect of a relatively strong Ti addition to an alloy containing Cu has a negligible influence on the crack resistance. Generally, the results from Figures 3 and 4 show that hot tearing is very dependent on alloy composition.

Comparing the hot tearing sensitivity of alloys in group B (Cu content in a range of 0.3 to 1.28 pct) to alloys in group A with 0.34 wt pct Cu shows a higher value of HTS for the B alloys. Thus, B-type alloys show more sensitivity to hot tearing than A-type alloys, again indicating the negative role of copper addition on the hot tearing tendency. However, all B alloys contain small additions of Zr.

B. *Hot Tearing Susceptibility and Microstructure*

A number of investigations at crack locations were carried out to study the relation between the HTS and the microstructure of the alloys in Table I. Figures 5(a)

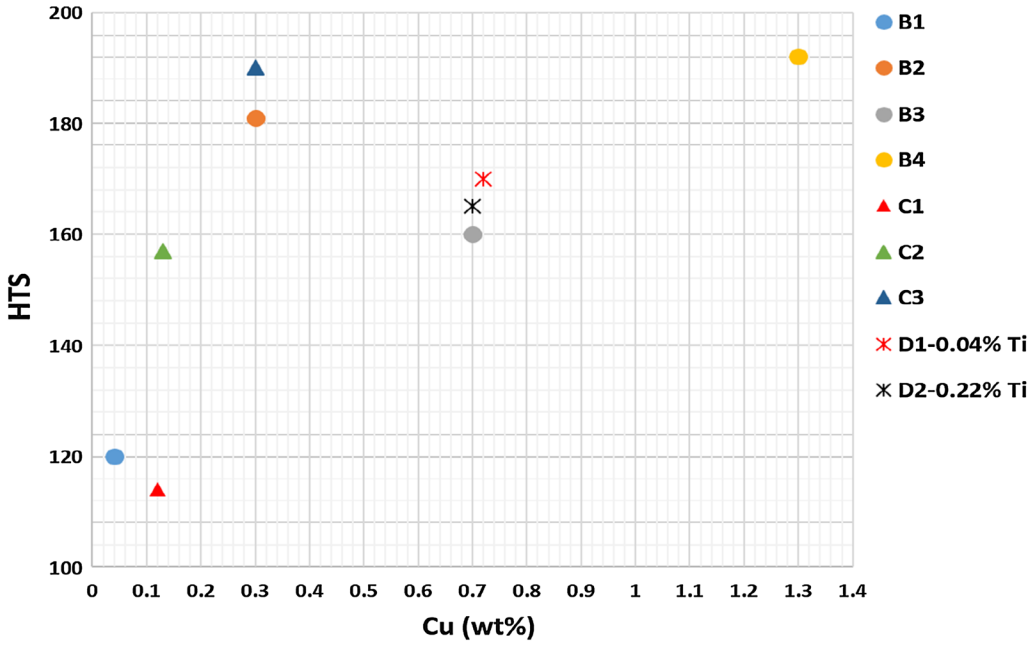

Fig. 4—Hot tearing susceptibility as a function of Cu content.

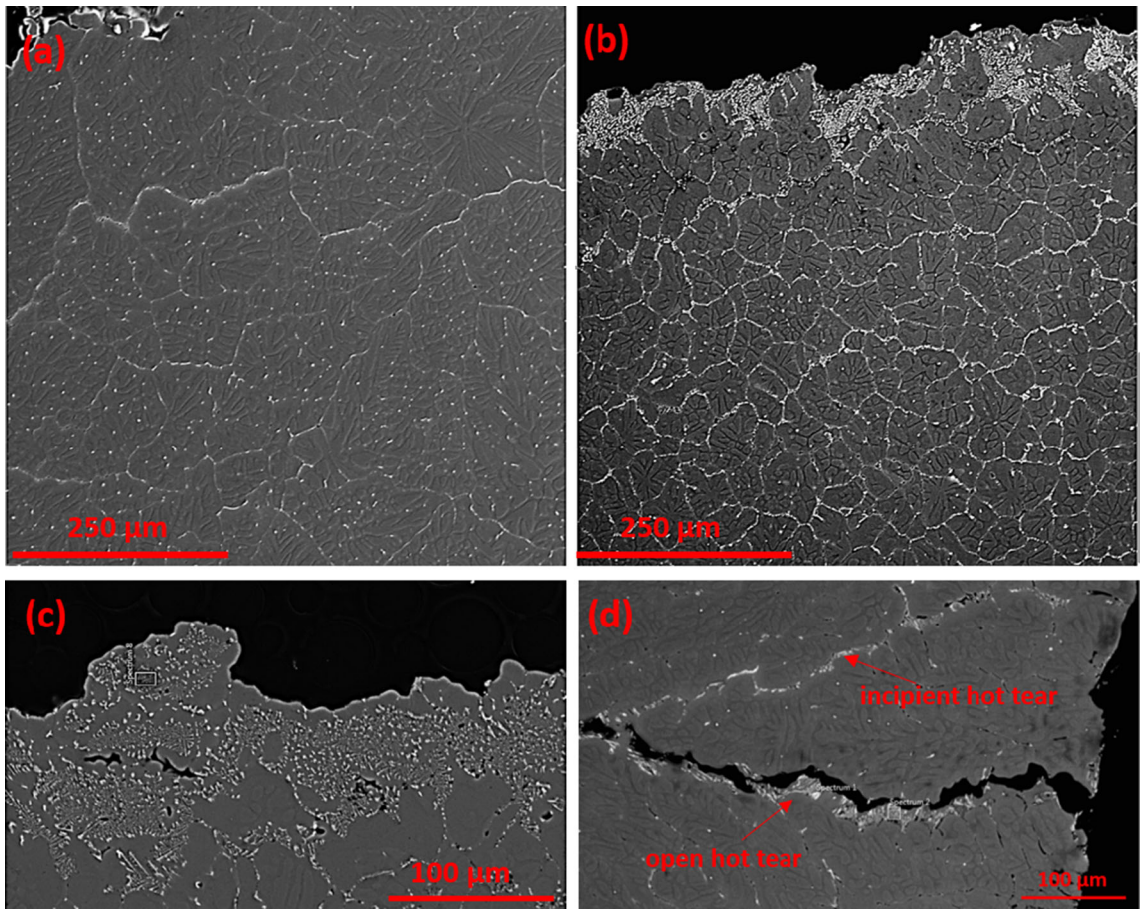

Fig. 5—SEM image from hot- tearing regions of: (*a*) alloy A2, (*b*) alloy A3, showing the higher number of intermetallic phases ($Al_6(Mn, Fe)$) in A3. (*c*) Magnified image of alloy A3; the main crack occurred at the upper edge of the eutectic area. (*d*) Alloy A1 showing crack at the edge of the eutectic structure.

and (b) show the morphology and distribution of eutectics from alloys A2 and A3 with low and high Fe content, respectively, at the hot tear location in rod A (the longest rod in Figure 1). As can be seen, the quantity of interdendritic liquid clearly varies for these two alloys. A larger amount of eutectic is seen in alloy A3, mainly accumulated close to the crack edge. This eutectic liquid was probably sucked in to heal the crack at a late stage of solidification, but subsequently a still crack formed at the edge of the solidified eutectic. Further away from the crack, intermetallic phases are distributed more homogenously along the grain boundaries in the alloy with higher Fe content, A3. The EDX analysis of these phases showed a composition corresponding to Al_6(Mn, Fe). Close to the crack locations in the large eutectic areas, discontinuous short cracks that appear similar to shrinkage porosity are observed, Figures 5(b) and (c).[23] Figure 5(d) shows an open hot tear in alloy A1, which was formed by rupturing a segregated liquid film. In addition, an incipient tear (solute-rich path) is found in Figure 5(d), which is evident of crack healing with eutectic liquid.[5,23]

Results from fracture surface investigations at the sprue side of rod A for alloys A2 and A3 are shown in Figure 6. The fracture surfaces include intermetallic phases. Some frozen eutectic liquid also covers the surface of primary dendrites and grain boundaries. A comparison of the surface of alloys A2 and A3 with 0.12 and 0.2 wt pct Fe clearly shows a higher number of intermetallic phases for the higher Fe content, Figures 6(c) and (d).[14,24]

Figure 7(a) shows Al_6(Mn, Fe) phases that have been extracted using a deep etching technique with dissolution of matrix in alloy A3. Al_6(Mn, Fe) phases are seen as a three-dimensional network with a similar structure to particles on the fracture surface of alloy A3,

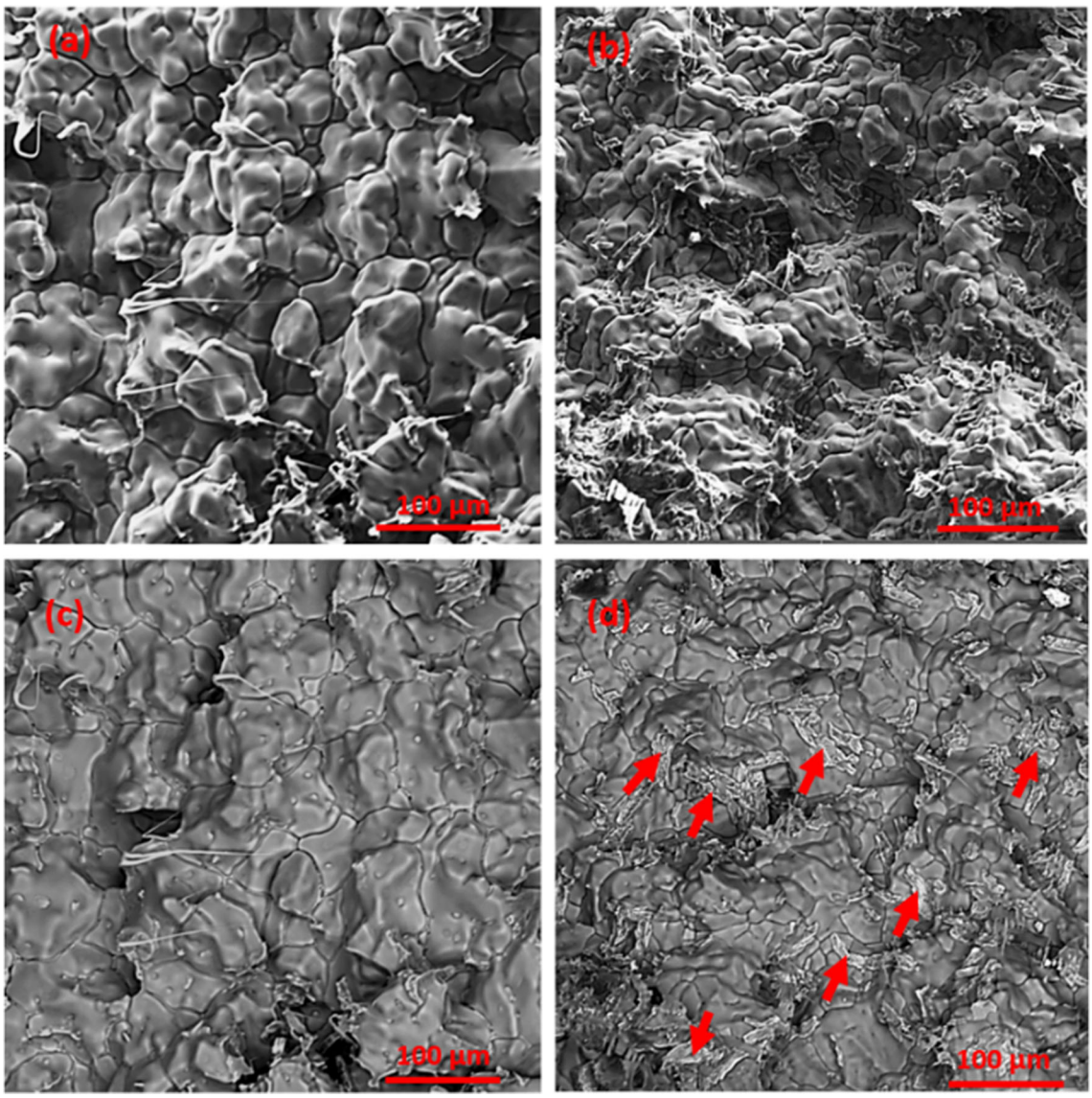

Fig. 6—SEM secondary electron micrographs from fracture surfaces of (*a*) alloy A2, (*b*) alloy A3. Backscattered electron images from fracture surfaces of (*c*) alloy A2, (*d*) alloy A3, showing the same areas as in (a) and (b) with arrows pointing to the particles.

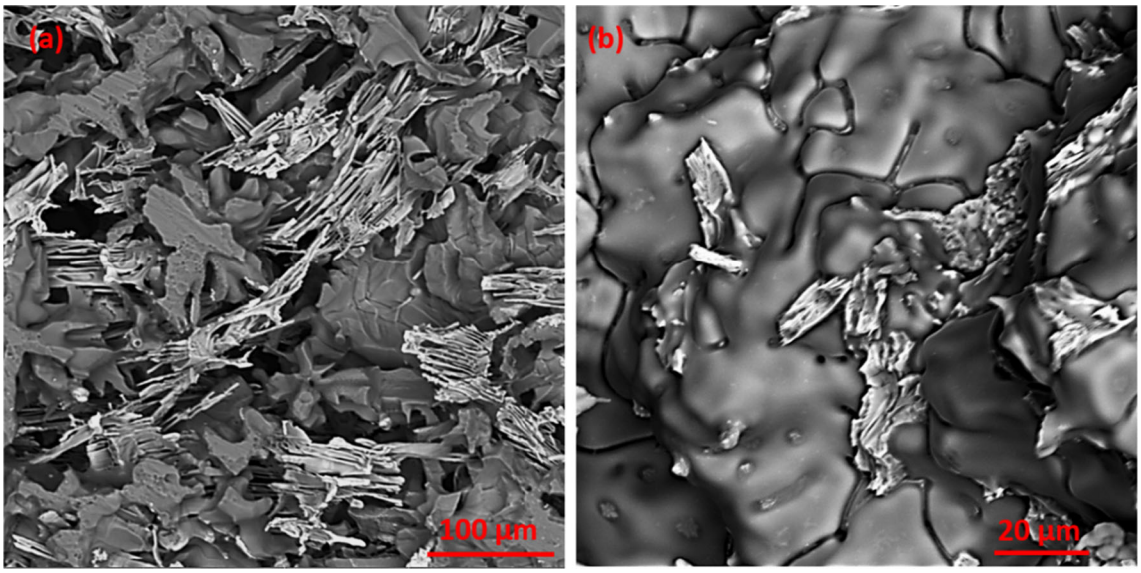

Fig. 7—SEM image showing the Al_6(Mn, Fe) phases in alloy A3: (*a*) three-dimensional intermetallic phases network after deep etching, (*b*) at fracture surface.

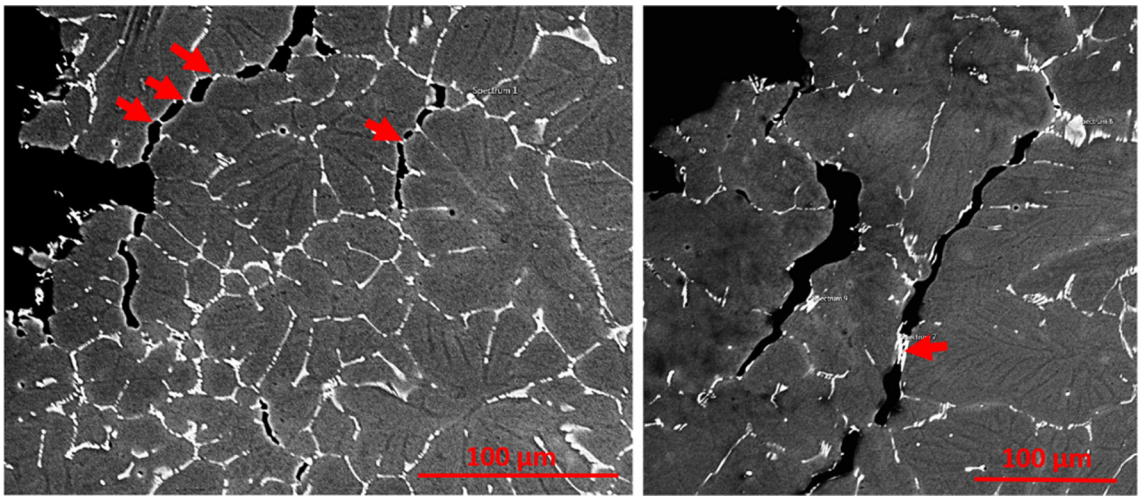

Fig. 8—Al_6(Mn, Fe) phases have bridged the grains in alloy A4 (marked by arrows).

Figure 7(b). This confirms that the observed particles on the fracture surface of alloy A3 in Figure 6(d) are Al_6(Mn, Fe) phases.

Figure 8 shows SEM observations from the strained areas close to hot tearing locations of alloys with increased Fe content (A4, 0.29 pct Fe). There is bridging between grains with platelet phases of Al_6(Mn, Fe). This can also be seen in Figure 7 with dendrites that are connected in some locations through Al_6(Mn, Fe) phases.

Figures 9 and 10 show the differences that occur when the Cu content is increased from 0.34 to 0.78 wt pct in alloys A4 and A5. Comparison shows a significant change in the microstructure in the hot tearing region. First, in the higher Cu content alloy, A5, a large amount of shrinkage porosity was observed, which can act as stress concentrator and initiate cracking[5,25] (Figures 10(a) and (b)). Second, an equiaxed structure with more developed dendrites in the interior of the grains is formed in alloy A5 (Figure 10(c)) compared to the more globular dendrites in alloy A4 (Figure 9(c)).

Figure 11 shows results from the hot tear location of alloy A6 with 0.07 wt pct Zr. A number of thin spikes have formed on the tear surface, Figure 11(a), which were not observed in the ruptured surfaces of the other investigated alloys. These spikes are probably signs of solid bridging between dendrites that were elongated before fracture occurred. They could also be deformation during solidification of the last remaining interdendritic liquid.[9] The morphology of alloy A6 also reveals a globular structure with less dendritic characteristics, Figure 11(b), compared to the A4 and A5 alloys in Figures 9(c) and 10(c), respectively. These observations show that adding Zr to a level of 0.07 pct has changed

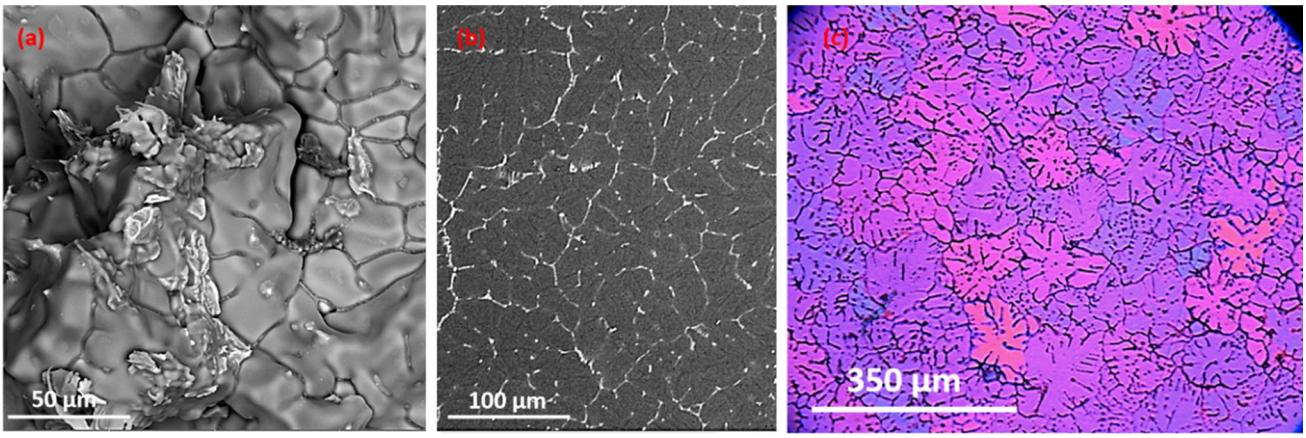

Fig. 9—Microstructure of the alloy A4 with 0.34 pct Cu: (*a*) SEM image of fracture surface, (*b*) SEM image close to crack spot, (*c*) grain morphology close to crack spot.

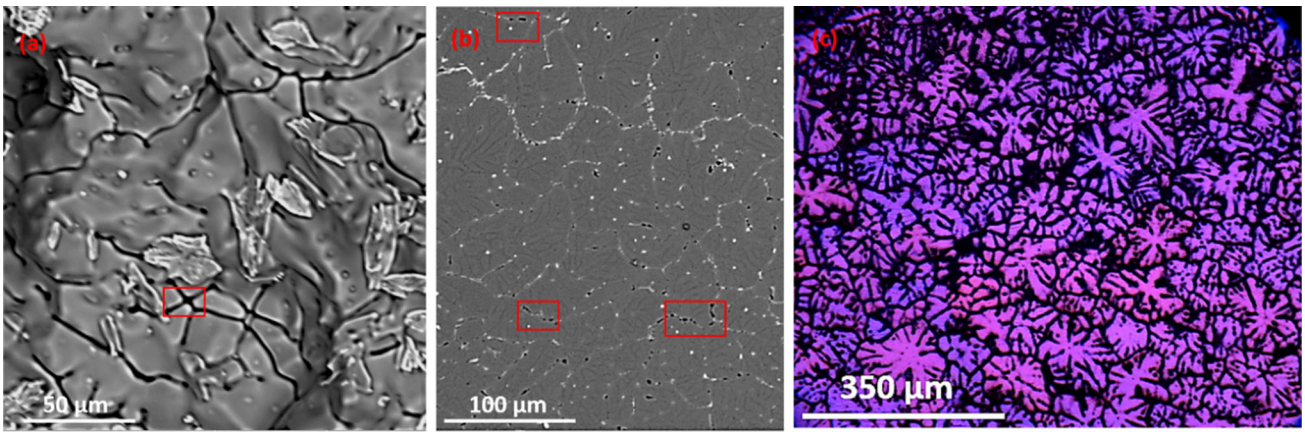

Fig. 10—Microstructure of the alloy A5 with 0.78 pct Cu: (*a*) SEM image of fracture surface, (*b*) SEM image close to crack spot, (*c*) grain morphology close to crack spot. Rectangular regions show the porosity.

the hot tearing behavior as well as the microstructure to more globular grains.

Grain sizes for the group A alloys were measured. Alloys A3, A4, A5, and A6 have a grain size of about 80 μm, while grains for low Fe alloys A1 (non-grain refined) and A2 (grain refined) are larger with sizes of 160 and 100 μm, respectively.

Figure 12 shows the grain morphology at hot tear locations for the B alloy group in Table II containing Cu content in the range of 0.3 to 1.28 wt pct. Coarse and partly columnar grains have been formed in all B alloys. In addition, the number of secondary phases has increased with increasing Cu content from alloy B1 to alloy B4. The EDX analysis of the secondary phases reveals that they correspond to two types of phases: $Al_6(Mn, Fe)$ and Al_2Cu. The Al_2Cu phase has been mostly formed with the appearance of a divorced eutectic. Grain size measurements showed that the different amount of Cu added does not affect grain size and morphology. The low levels of boron (Table II) in these alloys indicate that the grain refiner added to these alloys is at a low level.

Interesting observations could be made on the macroscale regarding solute-segregated zones around partially hot-torn positions. A stronger effect was observed in the long rods compared to the shortest rods, but it could also be seen in the large segregated zone in the ball parts of the alloy D1 (Figure 13).

C. *Effect of Eutectic Fraction*

Since the HTS can be related to the fraction of eutectic liquid, it is important to examine the evolution of the liquid fraction in the alloys.[10] Alloys from groups A and B were cast using the DC casting simulator to reproduce the solidification condition in as-cast ingots. The microstructure obtained at different distances from the chill surface for alloys A2, A3, and D1 is shown in Figure 14. It can clearly be seen that the $Al_6(Mn, Fe)$ eutectics appear in a larger fraction along

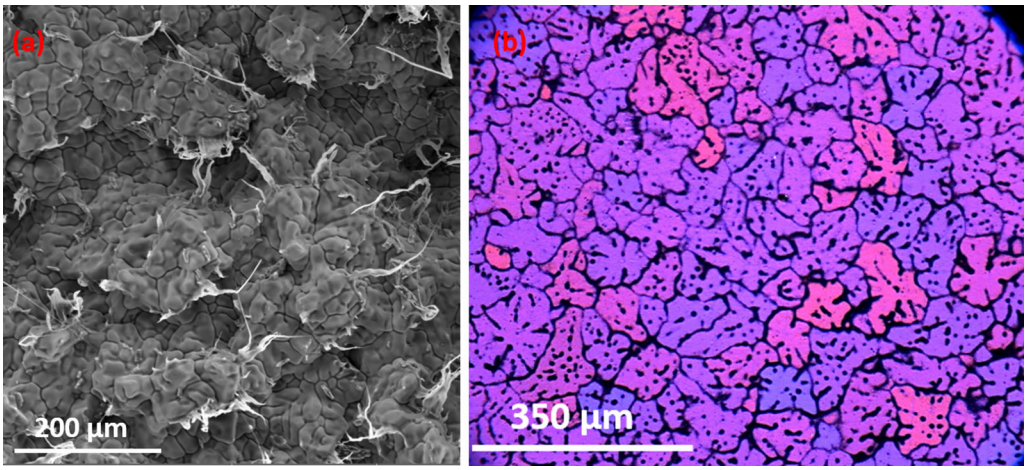

Fig. 11—Microstructure of the alloy A6 with 0.07 wt pct Zr: (*a*) Backscattered image of fracture surface, (*b*) grain morphology at crack spot.

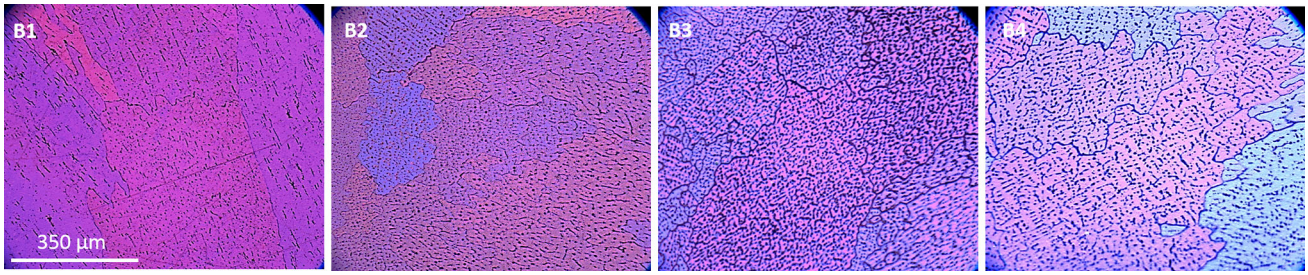

Fig. 12—Grain morphology in hot tearing regions for the B alloy group.

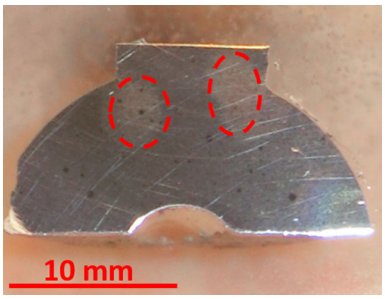

Fig. 13—Macrostructure from the longitudinal cut of a ball part of alloy D1. Rings mark the segregated zones (light areas).

the whole sample in alloy A3 with 0.2 wt pct Fe, compared to alloy A2 with 0.12 wt pct Fe. Quantitatively, the volume fractions of eutectic phases were evaluated as 0.22, 0.3, and 0.41 pct for alloys A2, A3, and D1, respectively. Figure 15 illustrates the hot tearing tendency *vs* the volume fraction of eutectics. It can be seen that increasing the $Al_6(Mn, Fe)$ eutectics from 0.22 to 0.3 pct for alloys A2 and A3, respectively, has reduced the hot tearing tendency. However, the highest hot tearing tendency was obtained for alloy D1 with the highest amount of eutectic (0.41 pct). These opposite trends illustrate the complexity of the hot tearing phenomenon and indicate that different mechanisms need to be considered.

D. *Mold Temperature Effect*

Thermo-mechanical factors based on the stress-strain rate during casting play an important role in hot tearing.[1] Thus, experiments using the CRC technique with different mold temperatures were carried out to examine the hot tearing behavior of alloys at different strain rates during casting. Table IV shows the HTS of alloys A1 and D1 from two different mold temperatures, 330 °C and 500 °C, inducing higher and lower strain rates, respectively. While the HTS values for alloy A1 decreased with increasing mold temperature, a weak opposite trend occurred for alloy D1. The result for D1 is interesting as in general HTS is expected to decrease with increasing mold temperature, however, the difference is small and the conclusion is that the mold temperature does not influence the HTS for alloy D1 in this limited range. The HTS values are clearly higher for the D1 alloy than for alloy A1.

IV. DISCUSSION

Hot tearing is very dependent on alloy composition, and small additions of alloying elements may have a large impact on the HTS of the alloys. In the literature, HTS has been associated with factors such as the solidification interval, microstructure development, eutectic feeding ability, and stress–strain induced during

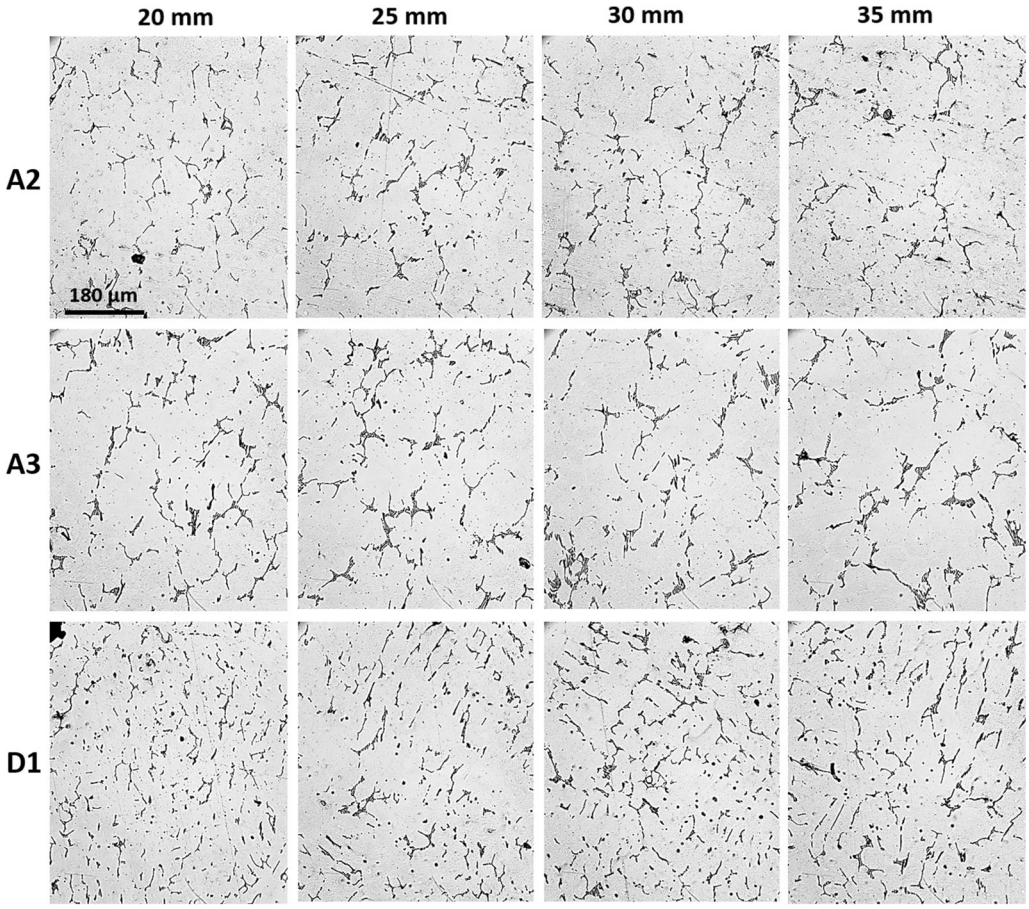

Fig. 14—Microstructure of DC simulator samples at various distances from the bottom for alloys A2, A3, and D1.

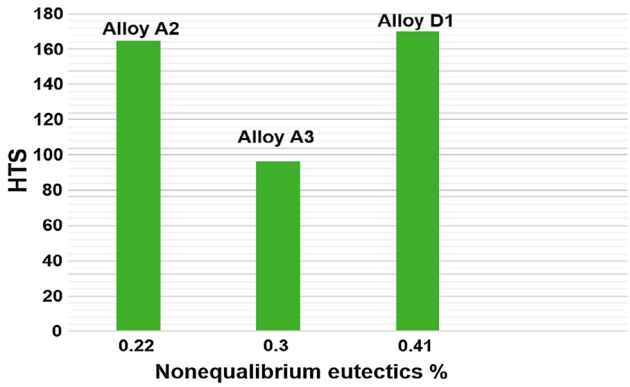

Fig. 15—Hot tearing susceptibility for alloys A2, A3, and D1 ordered by fraction eutectics.

solidification.[1,4,5,26] The correlation between these factors, alloying additions, and HTS for AA3000 alloys is discussed in what follows.

A. *Effect of Fe Addition*

Figure 3 shows that decreasing the Fe level below 0.2 wt pct has a significant impact, increasing the HTS in AA3000 alloys. However, several previous studies have presented contradictory results regarding the role of Fe addition in the hot tearing tendency of Al alloys. Some claim that the hot tearing tendency decreased with increasing Fe content for 6xxx,[3,13] 2xxx,[25] and foundry Al-Si alloys.[27] However, an increase in hot tearing with Fe addition was reported for 2xxx[10] and 6xxx Al alloys.[11] The negative effect of Fe content on hot tearing formation was described as follows: Increasing the Fe content promotes the precipitation of Fe-intermetallic compounds, impeding liquid feeding during the crack healing process.[10] In addition, some have stated that Fe addition increases the number of needle-shaped intermetallic phases, which can result in fragile grain boundaries, and therefore, a higher cracking tendency.[11] Nevertheless, the research reported in this paper shows a beneficial effect of increased Fe from 0.14 to 0.2 wt pct, as it decreased the HTS, Figure 3.

Figures 6 and 14 from fracture surfaces and samples made with the DC simulator, respectively, show that increasing the Fe content, as in alloy A3, resulted in the formation of a larger amount of $Al_6(Mn, Fe)$ phases. Figures 7 and 8 from the three-dimensional structure of $Al_6(Mn,Fe)$, and the hot tearing region, respectively, show that aluminum grains are bonded by $Al_6(Mn, Fe)$ phases. In DTA analysis and Bridgman solidification of similar alloys,[28,29] it was shown that $Al_6(Mn, Fe)$ phases formed early and in parallel with Al dendrites,

Table IV. HTS of the Alloys from Different Mold Temperatures

Alloys	Mold Temp 1 (°C)	HTS 1	Mold Temp 2 (°C)	HTS 2
A1	330	156	500	133
D1	330	170	500	182

which may reinforce the microstructure by bridging the gaps between primary dendrites. This will strengthen the alloy against hot tearing formation during liquid–solid contraction in the same way as has been proposed for the β phase in 6xxx[3] and foundry alloys.[27] Therefore, it can be concluded that Fe additions up to the level of 0.2 wt pct enhance hot tearing resistance in AA3000 alloy owing to precipitation of primary Al_6(Mn, Fe) phases improving the bridging ability between the grains. Thus, Al_6(Mn, Fe) phases play a very important role in hot tearing in this type of alloy; decreasing the Fe content below 0.2 wt pct can cause problems.

It is believed that alloys are more prone to hot tearing with a larger solidification interval, as they spend more time in a vulnerable region. According to the Al-Fe phase diagram, Fe has a very low solubility in Al (0.04 wt pct),[30] thus Fe additions at this level will not change the solidification interval. Thus, changing the Fe content only results in the formation of a different amount of intermetallic phases, Al_6(Mn, Fe), and not in different liquid feeding conditions. These phases are also formed earlier at higher Fe content, which might be the most important factor for the occurrence of bridges.

B. *Effect of Cu Addition*

In binary Al-Cu alloys, the highest cracking tendency is seen in a range of 0.7 to 1 wt pct Cu (lambda curve),[1] but HTS data for multicomponent commercial AA3000 alloys have not been available previously. In the present paper, a similar increase in HTS with Cu additions from 0.3 to 1.2 wt pct was proven (Figure 4). In addition, a Cu addition to the base A alloy A3 to a level of 0.78 wt pct Cu (A5), significantly increased HTS (Figure 3). The detrimental effect of Cu addition to an AA 6000 alloy was discussed in Reference 13, where the addition of 0.16 wt pct Cu significantly increased HTS. The following section discusses the generally negative influence of Cu.

The effect of adding Cu can be seen in Figure 10, which shows the fracture surface and microstructure of alloy A5. A noticeable number of pores between grains and dendrite arms can be observed. It has also been reported in Reference 14 that porosity increases with increasing Cu content to a level of 3.5 wt pct. It is well-known that porosity causes stress concentration and acts as a crack initiator.[5,25] The change in dendritic morphology with increased Cu content, seen when comparing Figures 9 and 10, can explain the porosity as the result of insufficient interdendritic liquid feeding in a more branched structure.[10,25] Also, this dendritic morphology weakens the ability of a system to form solid bridges between the dendrites.[25] This, coupled with the longer solidification interval and the strong growth restricting effect of Cu, can explain why the HTS generally increases with increasing Cu content. This is clear from both Figures 3 and 4, and is also well-known from other papers, such as.[1,13] The increase in solidification interval and dendritic morphology has been quantified in DTA experiments in References 28 and 29 for these alloys.

In the CRC technique, the mold temperature, MT, can be used to change the cooling rate. Decreasing the MT decreases the solidification time and increases the stress-strain rate in the rods. In addition, increased solidification time is related to higher MT, and provides a longer time for eutectic liquid to refill the cracks. It can, therefore, decrease the hot tearing severity.[7,25] Figure 15 displays variations in HTS following changes in MT and shows that the HTS value is reduced for alloy A1 when the MT is raised. More surprisingly, a slight increase in HTS was observed from increasing the MT for alloy D1. The latter observation contradicts results in References 1 and 25 that show a general reduction of HTS with increasing MT. The current results indicate that decreasing the strain rate during casting did not improve the hot tearing resistance for the alloy D1. This alloy is the industrial base alloy and contains 0.78 wt pct Cu, and has a relatively high eutectic fraction (Figure 15). All alloys containing this amount of Cu have been shown to have high HTS values, that is, they have very high crack sensitivity. Common theories say that alloys with high eutectic fractions are less prone to cracking due to adequate liquid feeding during shrinkage in solidification,[14,25] but obviously this particular alloy composition, D1, does not provide enough eutectic for cracks to heal. Paper 23 showed that initial cracking can start at a very early stage of solidification, for example in a solid fraction of 0.3. Although the residual liquid phase can infiltrate to heal the crack, a new crack can open up at the same position. This time, however, the crack cannot be healed due to insufficient eutectic feeding and thus leads to a hot tear. Thus, the hot tearing mechanism is controlled not only by the stress-strain rate, but also by how the eutectic liquid can infiltrate.[23] This phenomenon can possibly be observed in Figures 5(b) through (d), where healing of an original crack by a large amount of eutectic has been followed by a new crack along the first solidified eutectic edge.

The present results demonstrate that presence of eutectic liquid at low temperatures for the Cu-containing alloys can cause a higher HTS. Based on the finding in this work, it can be said that hot tearing behavior is more complex in Cu-containing alloys such as alloys B and D in Tables I and II, compared to the A alloys. This also fits well with experience from DC casting of ingots in industry. Cracking in this alloy, D1, seems to occur

randomly but with a high frequency, which suggests that various parameters are involved in the crack formation. An analysis of the crack region in large ingots revealed a large fraction Al_2Cu phase,[28] showing a strongly nonequilibrium amount of eutectic. Another interesting observation in this context is Figure 13, where large zones with macro-segregation occur at stress concentration points. This was only observed in the Cu alloys. In paper 17 CRC was complemented by load measurements to analyze an alloy of similar composition to D1. It was found that a strong increase in load occurred very late, at a solid fraction of 0.98, compared to other alloys, indicating the existence of liquid films late in the solidification process.

It should be noted that the microstructure investigation performed in the DC simulator (Figure 14) revealed grains with columnar structure in the D1 alloy but not in the A2 or A3 alloys. Large and partly columnar grain also occurred in the CRC experiments for the B alloys, probably due to a lower level of grain refiner additions in this group. It is likely that alloys with columnar morphology are less able to accommodate induced strain during the last stage of solidification compared to equiaxed grains, and thus show a high tendency to cracking.[1] The high HTS in alloy D1 can, therefore, partly be attributed to its columnar morphology even though this alloy is grain refined to a high level.

C. *Effect of Ti and Zr Addition*

Reference 31 states that Ti decreases the Mn solubility in Al for 3xxx alloys. More precipitation of primary Al_6(Mn, Fe) phases and fewer eutectic phases can, therefore, be expected in alloys with higher Ti content. This can contribute to the larger amount of eutectic found in alloy D1 than in alloy A3 as shown in Figures 14 and 15. It can also be concluded that higher Ti content in alloy A3 has favored primary Al_6(Mn, Fe) precipitation, improved the bridging and thus the hot tearing resistance (Figure 3).

Moreover, Figure 4 showed that alloys D1 and D2 with 0.04 and 0.22 wt pct Ti, respectively, have approximately the same HTS value. This means that for these crack-sensitive Cu-containing alloys the known favorable effect of Ti on HTS[1] does not apply.

The hot tearing index in Figure 3 illustrates that Zr addition to a level of 0.07 wt pct as in alloy A6 significantly raises the HTS. In addition, Figure 11, from the fracture surface of the same alloy, indicates the presence of thin spikes, which are normally associated with freezing of the last interdendritic liquid during separation of the crack surfaces. Thus, addition of Zr has increased the HTS and altered the hot tearing behavior at the end of solidification.

V. CONCLUSION

The hot tearing behavior of AA3000 alloys containing Cu, Ti, and Zr was investigated using a CRC mold technique. It was found that Fe and Cu additions have a dominant impact on the HTS of AA3000 alloys compared to Ti and Zr. Decreasing the Fe content below 0.2 wt pct significantly reduces hot tearing resistance. Phase characterization has shown that Fe addition up to 0.2 wt pct promotes the precipitation of the primary Al_6(Mn, Fe) phase, which results in early bridging of dendrites, and reinforces the structure during coalescence. Thus, Fe additions improve the hot tearing resistance.

Cu content in a range of 0.3 to 1.2 wt pct has a detrimental effect on hot tearing resistance. Cu additions enlarge the solidification interval, giving a higher fraction of eutectic at the end of solidification. It also changes the morphology to more branched dendrites and partly columnar structures and increases the shrinkage porosity.

Zr and Ti additions weakly enhanced or reduced the hot tearing severity, respectively. The effect of grain refinement on HTS in alloys containing Cu at about 0.7 wt pct was negligible.

ACKNOWLEDGMENTS

The authors acknowledge Sweden's Innovation Agency for their financial support and Kubikenborg Aluminium AB and Gränges Sweden AB for providing material, OES analysis, and important input regarding industrial practices.

REFERENCES

1. S. Li and D. Apelian: *Int. J. Metal Cast*, 2011, vol. 5, pp. 23–40.
2. Q.L. Bai, Y. Li, H.X. Li, Q. Du, J.S. Zhang, and L.Z. Zhuang: *Metall. Mater. Trans. A*, 2016, vol. 47A, pp. 4080–91.
3. L. Sweet, M.A. Easton, J.A. Taylor, J.F. Grandfield, C.J. Davidson, L. Lu, M.J. Couper, and D.H. Stjohn: *Metall. Mater. Trans. A*, 2013, vol. 44A, pp. 5396–5407.
4. D.G. Eskin and L. Katgerman: *Prog. Mater. Sci.*, 2004, vol. 49, pp. 629–711.
5. D.G. Eskin and L. Katgerman: *Metall. Mater. Trans. A*, 2007, vol. 38A, pp. 1511–19.
6. M. Easton, J. Grandfield, D. StJohn, and B. Rinderer: *Mater. Sci. Forum*, 2006, vols. 519–521, pp. 1675–80.
7. F. D'Elia, C. Ravindran, D. Sediako, K.U. Kainer, and N. Hort: *Mater. Des.*, 2014, vol. 64, pp. 44–55.
8. M. Uludağ, R. Çetin, and D. Dispinar: *Metall. Mater. Trans. A*, 2018, vol. 49A, pp. 1948–61.
9. M. Rappaz, I. Farup, and J.-M. Drezet: *Light Metals*, TMS, Warrendale, 2000, pp. 213–22.
10. H.K. Kamga, D. Larouche, M. Bournane, and A. Rahem: *Mater. Sci. Eng.*, 2010, vol. 527, pp. 7413–23.

11. H. Nagaumi, S. Suzuki, T. Okane, and T. Umeda: *Mater. Trans.*, 2006, vol. 47, pp. 2821–27.
12. D. Viano, D. St John, J. Grandfield, and C. Cáceres: *Light Metals*, TMS, Warrendale, 2005, pp. 1096–73.
13. L. Stermann and M. Iraizoz: *Light Metals*, TMS, Warrendale, 2018, pp. 389–95.
14. D.G. Eskin and L. Katgerman: *Mater. Sci. Eng.*, 2006, vol. 420, pp. 1–7.
15. H. Nagaumi, X. Guanxia, Z. Zheng, and M.A. Yuli: *Mater. Sci. Forum*, 2014, vols. 783–786, pp. 300–306.
16. L. Sweet, J.A. Taylor, M.J. Couper, and M. Easton: *Mater. Sci. Forum*, 2011, vol. 693, pp. 217–23.
17. A. Nordmark, K. Ellingsen, A. Johansson, M. M'Hamdi, A. Kvithyld, A. Marson, and A. Azar: *Mater. Sci. Forum*, 2014, vols. 794–796, pp. 95–100.
18. S. Lin, C. Aliravci, and M.O. Pekguleryuz: *Metall. Mater. Trans. A*, 2007, vol. 38A, pp. 1056–68.
19. J. Song, F. Pan, B. Jiang, A. Atrens, M.X. Zhang, and Y. Lu: *J. Magnes. Alloys*, 2016, vol. 4, pp. 151–72.
20. G. Cao and S. Kou: *Mater. Sci. Eng. A*, 2006, vol. 417, pp. 230–38.
21. T. E. Quested: Ph.D. thesis, Cambridge University, UK, 2004.
22. A.K. Gupta, P.H. Marois, and D.J. Lloyd: *Mater. Charac.*, 1996, vol. 37, pp. 61–80.
23. H. Yamagata, H. Tachibana, S. Kijima, M. Adachi, and S. Koiwai: *Adv. Mater. Process. Technol.*, 2018, vol. 4, pp. 480–92.
24. D.G. Eskin and L. Katgerman: *Mater. Sci. Forum*, 2007, vols. 561–565, pp. 995–99.
25. A.M. Nabawy, A.M. Samuel, F.H. Samuel, and H.W. Doty: *J. Mater. Sci.*, 2012, vol. 47, pp. 4146–58.
26. Y.D. Haung, J. Song, S.H. You, and N. Hort: *Conf. Solid. Process.*, 2017, vol. 6, Decennial, pp. 459–63.
27. L. Lu and A.K. Dahle: *Metall. Mater. Trans. A*, 2005, vol. 36A, pp. 819–35.
28. M.M. Jaradeh and T. Carlberg: *J. Mater. Sci*, 2011, vol. 27, pp. 615–27.
29. M. Jaradeh and T. Carlberg: *Metall. Mater. Trans. A*, 2007, vol. 38, pp. 2138–47.
30. A.S. Najafabadi: PhD thesis, McGill University, Canada, 1996, ISBN 0-612-12481-9.
31. G. Razaz, T. Carlberg: On the Dissolution Process of Manganese and Iron in Molten Aluminum, *Metall. Trans. A*, 2019, Published Online, ISSN 1073-5623.